Supplementary Materials for

Exceptional Convergence on the Macroevolutionary Landscape in Island Lizard Radiations

D. Luke Mahler,* Travis Ingram, Liam J. Revell, Jonathan B. Losos

*Corresponding author. E-mail: lmahler@ucdavis.edu

Published 19 July 2013, *Science* **341**, 292 (2013)
DOI: 10.1126/science.1232392

This PDF file includes:

Other Supplementary Material for this manuscript includes the following:
(available at www.sciencemag.org/cgi/content/full/341/6143/292/DC1)

Tables S1 and S2 as zipped archives (1232392s1.csv and 1232392s2.csv)

This PDF file includes:

Other Supplementary Materials for this manuscript include the following:

Tables S1 to S2 as zipped archives: [1232392s1.csv, 1232392s2.csv]

Materials and Methods

1. Data and Morphospace Estimation

We conducted our analyses using the morphological and phylogenetic data described in (*17*). Our sample included 100 of the 119 currently recognized species of *Anolis* from the main islands of the Greater Antilles (Cuba, Hispaniola, Jamaica, and Puerto Rico). These species were originally selected on the basis of the joint availability of morphological and phylogenetic data, but they nearly fully represent the phylogenetic and ecomorphological diversity of Greater Antillean anoles. For all but two unsampled species (both rare Haitian endemics for which molecular data are not yet available), we have included at least one ecologically and morphologically similar sibling species in our data set. Our study therefore nearly completely represents the evolutionary diversity of Greater Antillean anole ecologies and morphologies.

We used morphological data from the data set reported in (*17*). Those authors reported mean values for each trait for each species, sampling 7.9 specimens per species on average (range: 1-19). The outcome of any multivariate test for convergence will depend on the types of traits selected to define the morphospace, as well as the precision with which they were measured. Therefore, from the set of traits used in (*17*), we selected a subset of 11 accounting for the most ecologically important axes of morphological variation in *Anolis*, as assessed in prior studies: snout-to-vent length (SVL), tail length, femur length, tibia length, length of metatarsal IV, length of hindtoe IV, humerus length, radius length, length of foretoe IV, toepad lamella number for hindtoe IV, and toepad lamella number for foretoe IV. We chose these traits because they are known to correlate with habitat use and niche partitioning in Caribbean anoles, and they closely correspond to traits used in previous studies of ecomorphological convergence in anoles (*14*), but we note that additional ecomorphological characters such as mass were not included because they were not available for all species. A single investigator (D.L.M.) made all measurements, discarding and re-taking the first third to ensure that repeatability estimates were comparable across the sample (*17*).

We conducted all phylogenetic comparative analyses using the ultrametric maximum clade credibility (MCC) mtDNA phylogenetic tree for Greater Antillean anoles from (*17*). Chronograms in that study were estimated by partitioned Bayesian analysis of a ~1,500 bp, six-gene fragment of mitochondrial DNA, assuming an uncorrelated relaxed molecular clock model, using the program BEAST (*35*). To assess the effect of phylogenetic uncertainty on our results, we repeated our analyses on a sample of 100 trees from the posterior distribution of ultrametric mtDNA phylogeny estimates from (*17*). Although these phylogenies were estimated using mitochondrial data, we note that a multilocus nuclear study of anole relationships based on less comprehensive taxon sampling (61 Greater Antillean spp.) has yielded topologically similar estimates of *Anolis* phylogeny (*36*). While the sampling for this nuclear DNA phylogeny is insufficient to test for convergence among entire Greater Antillean island faunas, we used it to confirm that both nuclear and mitochondrial DNA *Anolis* phylogenies yield similar models of trait evolution. To test this, we conducted convergence analyses on 61-species data sets using both types of phylogenies, obtaining qualitatively identical convergence results (Materials and Methods, Section 5a). The absolute timing of anole diversification in the

Greater Antilles remains poorly known, but we rescaled all trees to a crown age of 50 Ma so that estimates of evolutionary parameters would be in roughly appropriate units (*14*).

To generate a morphospace for Greater Antillean anole species, we first size-corrected all shape trait measurements using phylogenetic regression on SVL (*37*) in the R software package 'phytools' (*38*). We then conducted a phylogenetic principal component analysis (pPCA) (*37, 38*) on the covariance matrix of SVL and shape residuals to obtain evolutionarily orthogonal axes of morphological trait variation. We retained the first four pPC axes, which collectively explained 93% of variation, based on examination of an eigenvalue scree plot, and because these axes exhibited meaningful correlations with our original unrotated variables, while the remaining axes were difficult to interpret. For the analysis based on the MCC tree, we report the trait loadings, eigenvalues, and relative variances explained for our pPC axes in Table S1, and we report pPC scores in Table S2. As we used phylogenetic information to create our size and shape morphospace, these preparatory steps were included in our analyses of phylogenetic uncertainty. pPCA eigenvalues and loadings varied slightly, but were very similar across phylogenies (data available upon request).

2. Fitting Models of Continuous Trait Evolution, and Simulating Null Morphospaces

To evaluate whether the extent of convergence in Greater Antillean *Anolis* is exceptional, we compared empirical convergence statistics to null distributions generated by evolutionary simulation. We simulated data separately for each trait axis using whichever of a set of models of continuous character evolution best fit each axis (we refer to this as the "trait-specific" null model). First, we compared the fits of four models of continuous character evolution for each trait axis using small-sample corrected Akaike information criterion (ΔAIC_c) values (Table S3). We compared the following models: Brownian motion (BM), early burst (EB), time (TM), and lineage diversity (LD) (*17, 19*). The latter three models are generalizations of the BM model in which the rate of trait evolution may change as a function of time (for EB and TM) or island-specific species diversity estimates (for LD). The EB and TM models differ primarily in that the rate of evolution changes exponentially under the EB model, and linearly under the TM model.

Using the favored model for each axis, we next simulated 999 four-dimensional null trait data sets, using the MCC phylogeny and empirically-estimated generating parameters from the model-fitting exercise described above (generating parameters and other model details are reported in Table S3). We simulated data one axis at a time, then combined these axes to build our null morphospaces (note that when we repeated analyses using phylogenies from the posterior distribution, we also repeated this trait-specific model-fitting procedure).

For the sake of completeness, we simulated four additional sets of null morphospaces, this time simulating all trait axes under the same model (one set of morphospaces simulated under each of the BM, EB, TM, and LD models of evolution; parameter estimates are also found in Table S3). For all convergence tests, we obtained significant results that were qualitatively identical to those presented in the main text using data generated under all of these alternative models (see Materials and Methods, Sections 3 and 4d, below). We did not simulate using a multivariate model of trait evolution, because the axes of our empirical morphospace are geometrically orthogonal and evolutionarily uncorrelated, but we note that for data sets for which individual traits

exhibit evolutionary correlations, it would be appropriate to simulate null data with the estimated correlation structure. We fit models and conducted simulations using the R packages 'ape' (*39*), 'geiger' (*40*), 'phytools' (*38*), and 'surface' (*20*).

3. Testing for Among-Island Faunal Similarity

We tested for species-for-species matching among the four Greater Antillean islands by comparing an empirical among-island species similarity statistic to a simulated evolutionary null distribution. For each species in the Greater Antilles, we recorded the Euclidean distance to its nearest neighbor in morphospace from each of the other three islands. To quantify average among-island faunal similarity with a single metric, we calculated the island-weighted average of all among-island nearest neighbor distances (NND, calculated by first averaging among-island nearest neighbor distances for all species occurring within each island, and then averaging these four values). We then calculated the same set of distances for the simulated morphospace data sets described above, and compared the empirical among-island matching statistic to this null distribution to test whether Greater Antillean anoles exhibit exceptional faunal similarity. We found significant evidence for exceptional faunal similarity whether null data sets were simulated using the trait-specific null models or any of the single models (BM, EB, TM, and LD; Fig. S1). We also consistently found exceptional faunal similarity when we repeated the trait-specific null model simulations on the 100 phylogenies from the posterior distribution (mean NND = 0.31; $P \leq 0.007$).

4. Testing for Convergence on the Macroevolutionary Adaptive Landscape

We tested for convergent evolution in Greater Antillean *Anolis* using "SURFACE" (a recursive acronym for "SURFACE Uses Regime Fitting with AIC to model Convergent Evolution") (*20*), a method available as a package through the Comprehensive R Archive Network (CRAN) (http://cran.r-project.org/web/packages/surface/). The main purpose of this method is to identify lineages that have converged in phenotype without using *a priori* designations of ecomorphs. It builds upon two advances in phylogenetic comparative methods: the development of the "Hansen" model of adaptation of lineages to multiple distinct adaptive peaks (*21, 22*), and the use of stepwise algorithms such as MEDUSA (Modeling Evolutionary Diversification Using Stepwise AIC) (*23*) and trait MEDUSA (*24*) to locate regions of a phylogeny containing shifts in rates of diversification and trait evolution, respectively. SURFACE combines these features by allowing the data to dictate the placement of a peak shift on the macroevolutionary adaptive landscape [sometimes called a "selective regime shift" (*20-22, 27*)] on whichever branch of the tree most improves the AIC at each step. After adding as many adaptive peak shifts as are supported by the data, the method evaluates whether shifts in different lineages correspond to attraction to the same adaptive peak. Finally, the extent of convergence can be compared to a null model using simulation-based hypothesis tests.

In what follows, we describe the major features of this method and how we applied it to the *Anolis* data set. The SURFACE algorithm is described in greater detail in (*20*), which also presents the results of simulation tests that demonstrate desirable statistical properties and show that the tool can effectively recover the true adaptive landscape structure of data sets comparable in size to the anole data set used in the

present article. The simulation-based hypothesis test we employ here has good power to detect true convergence given multidimensional trait data for a moderate-sized radiation (n = 64 species), and has appropriate type I error rates when the generating model contains adaptive peak shifts but no true convergence.

4a. The Hansen model of continuous trait evolution

SURFACE proceeds by fitting a series of Hansen models of stabilizing selection around optimum phenotype values. Hansen models represent the adaptive evolution of a radiation on a Simpsonian macroevolutionary trait landscape (*3, 22, 27*). Within a radiation, different lineages may evolve under different selective regimes corresponding to distinct ecological niches (Simpson referred to these regimes as "adaptive zones"). On the macroevolutionary landscape, each such regime corresponds to an adaptive peak with a distinct optimum in trait space (*21, 22*). In the Hansen model, trait evolution is modeled as an Ornstein-Uhlenbeck (OU) process, whereby evolutionary change along each branch of a phylogenetic tree includes both a stochastic Brownian motion component and a deterministic tendency toward its adaptive optimum (*21, 22*). The parameters governing this process are the Brownian diffusion parameter (σ^2), the rate of adaptation towards the selective optima (α), and the positions of the optima (θ, one parameter per adaptive peak). The parameters of any Hansen model can be estimated using maximum likelihood (*21*). Past uses of the Hansen model have compared specific phylogenetic peak shift placements to test whether lineages are attracted to hypothesized adaptive peaks; SURFACE takes an alternative approach by allowing the data to dictate the selection of a Hansen model.

4b. Fitting a model with adaptive peak shifts to *Anolis* ecomorphology data

SURFACE consists of a two-phase stepwise procedure to test for multidimensional convergent evolution. In the "forward" phase, adaptive peak shifts are added to a Hansen model in a stepwise fashion to generate models representing successively more complex macroevolutionary adaptive landscapes. In the "backward" phase, convergent peaks are collapsed together, yielding a model from which we can estimate the prevalence of convergence in a given radiation.

We fit models of macroevolutionary convergence to the Greater Antillean *Anolis* data set, using the four morphological traits and phylogenetic information described above. We focus on estimating the macroevolutionary landscape with the MCC phylogeny, using simulations to test for exceptional convergence. We also fit models using 100 trees from the Bayesian posterior distribution to assess the sensitivity of our results to phylogenetic uncertainty, repeating the pPCA analysis for each tree as described above.

Phase 1: Identifying adaptive peak shifts

The starting point for the analysis is the single-peak Ornstein-Uhlenbeck model, in which all lineages are attracted to the same adaptive optimum. For a data set with m traits and n species, this model has $3m+1$ parameters: estimates of θ, σ^2, and α, for each trait, and a parameter representing the presence of the ancestral peak shift that affects the entire radiation. We used maximum likelihood optimization to estimate the parameters of this model (*21*) separately for each trait. We then added log-likelihoods across traits to

obtain an overall log-likelihood, assuming that the evolutionary parameters σ^2 and α are independent between traits. To measure model performance for comparison with models estimated in subsequent steps, we calculated the sample-size corrected AIC_c, where the sample size is the total number of trait values ($n \times m$).

Adaptive peak shifts are then added to this initial model, first by fitting all possible Hansen models with the ancestral shift at the root and a second peak shift placed at the origin of one of the $2n$-2 branches in the tree. We calculated log-likelihoods by adding across traits as before, then calculated AIC_c values for each candidate model. The number of parameters is defined as $k+(k'+2)m$, where k is the number of peak shifts in the model and k' is the number of adaptive peaks (during the forward phase all peaks are distinct, so $k'=k$). Adding a peak shift to the model thus increases the number of parameters by $m+1$, accounting for the complexity of both the adaptive landscape (m new estimates of θ) and the evolutionary history of the group (one new parameter corresponding to the placement of a new peak shift). The candidate model with the lowest AIC_c score is selected, and a peak shift is placed on the corresponding branch.

This process is iterated, with the positions of all previously added peak shifts fixed, and one new peak shift added at each step, until the AIC_c stops improving by at least a threshold value $\Delta AIC_c^* = 0$ [i.e., accepting all iterative model updates that improve the AIC_c, which generally results in good performance (*20*)].

Phase 2: Collapsing similar adaptive peaks

The forward phase of the analysis results in a Hansen model with k peak shifts on the tree, which correspond to $k'=k$ distinct adaptive peaks, each with an m-dimensional trait optimum. The backward phase uses a second stepwise AIC_c procedure to determine whether some of these adaptive peaks can be collapsed into convergent peaks reached by multiple shifts. We preserve the placement of the peak shifts on the phylogenetic tree, but allow multiple shifts to converge toward the same adaptive peak. While adding a peak shift increased the number of parameters by $m+1$, collapsing two adaptive peaks into one decreases the number of parameters by m. This is because the one parameter corresponding to the peak shift remains in the model, but m fewer optima are estimated as k' decreases by one. Thus, while reducing the number of optima means that the likelihood cannot improve when peaks are collapsed, the AIC_c can improve because fewer parameters are estimated due to the macroevolutionary adaptive landscape containing one fewer peak.

Starting with the Hansen model from the last step of the forward phase, we move through all pairwise combinations of adaptive peaks i and j, and re-fit the model after collapsing the two peaks into a convergent peak. This results in $k(k-1)/2$ candidate models, some of which may represent improvements over the previous model (i.e. $\Delta AIC_{c(ij)} < \Delta AIC_c^*$). We follow Ingram and Mahler (*20*) in allowing multiple pairs of adaptive peaks to be collapsed at each step, while ensuring that all peak collapses were compatible (i.e., all collapses meet the criterion $\Delta AIC_c < \Delta AIC_c^*$). This process of collapsing convergent peaks is iterated until no further collapses would improve the model by at least AIC_c^*.

4c. Visualizing the *Anolis* macroevolutionary adaptive landscape and testing for exceptional convergence

The SURFACE routine led to substantial improvements to the AIC_c of the Hansen model describing *Anolis* diversification compared to alternative models of trait evolution (the progress of stepwise model improvement with adaptive peak-shift addition and collapse is shown in Fig. S2; the final Hansen model is strongly favored over both the initial Hansen model ($\Delta AIC_c = 340.4$) and the non-convergent forward phase Hansen model ($\Delta AIC_c = 162.6$). For the MCC tree analysis, we identified shifts to $k = 29$ adaptive peaks on the four-dimensional macroevolutionary landscape during the forward phase, and collapsed these into $k' = 15$ distinct peaks during the backward phase (Table 1). The extent of convergence in the *Anolis* landscape can be measured as $c = 22$, the number of shifts toward adaptive peaks occupied by multiple lineages, and $c/k = 22/29 = 0.76$, the proportion of shifts that are convergent. In morphospace, species attracted to the same adaptive peak tended to cluster closely about their estimated adaptive optima (Fig. 2), as is expected for a radiation in which lineages diversify on highly similar macroevolutionary adaptive landscapes. This correspondence is particularly strong for pPC axes 1-3, which together explain the vast majority of the variation in our data (85%; Table S1).

The replicated adaptive radiation hypothesis predicts that allopatric lineages diversifying in similar ecological settings will evolve to occupy similar adaptive peaks. Thus, for convergent peaks in our final model, we asked whether convergence involved lineages from multiple islands. In the analysis based on the MCC phylogeny, seven of eight convergent peaks attracted lineages from multiple islands (Table 1; across phylogenies, this was true for 94% of convergent adaptive peaks, and all exceptions occurred on the large islands of Cuba and Hispaniola, where such lineages may have converged to the same peak while allopatric).

We also noted that while some non-convergent adaptive peaks contained species from multiple islands, the majority (five of seven) were endemic to a single island. The two "unique" lineages occupying multiple islands arose early according to our model, and colonized other islands without undergoing a peak shift (Fig. 2). Endemic unique lineages arose exclusively on the largest islands, Cuba and Hispaniola, in the model estimated for the MCC tree (this was also true for 96% of endemic unique lineages across phylogenies).

To test whether adaptation to unique peaks only on the larger islands may be attributed to the "area effect" from adaptive radiation theory (*1*), we conducted a phylogenetic randomization test. Holding the remainder of the parameters of our estimated model constant (i.e., phylogenetic topology, species island assignment, numbers of convergent and non-convergent peak shifts, numbers of convergent and non-convergent adaptive peaks, and number of shifts per convergent peak), we randomized the phylogenetic placement of peak shifts 100 times, and recorded the numbers of endemic unique lineages for each island. In this way we generated distributions of the expected number of endemic unique lineages for each island, given its evolutionary diversity; the "area effect" predicts that occupation of novel peaks is a function of evolutionary diversity (*1*), which is greater on larger islands in both anoles and other organisms (*14, 30, 31*). By comparing our empirical observations of the numbers of unique lineages on each island to these distributions, we confirmed that the tendency for unique anoles to be found only on large islands matches the predictions of the area effect (Fig. S3).

4d. Estimates of the *Anolis* landscape across phylogenies

Estimates of convergence on the macroevolutionary landscape were similar across sampled trees from the Bayesian posterior distribution of *Anolis* phylogenies (Table 1). Topological placement of adaptive peak shifts varied among phylogenies, although in general, groups of species tended to be attracted to peaks of similar composition across the posterior sample of trees. Because the topologies of alternative trees may differ, it is not straightforward to compare the topological details of peak shift placement across trees. Instead, we used a network approach to illustrate the major features of peak occupancy over our set of phylogenies. We constructed a graph with edges between species weighted proportional to the number of phylogenies in which they were attracted to the same adaptive peak (no edge is drawn between species that never shared a peak). We plotted this graph as a co-occurrence network (Fig. S4) with weighted edges. We used a Kamada Kawai force-based algorithm to aid in plotting this network such that species most frequently co-occupying adaptive peaks tend to be plotted near one another. We colored species according to traditional ecomorph assignment (although these assignments played no role in the estimation of Hansen models by SURFACE) to heuristically assess whether species classically considered as belonging to the same ecomorph also tended to occupy the same adaptive peaks. In general, members of the same ecomorph classes were attracted toward the same adaptive peaks in the fitted Hansen model (Fig. S4).

4e. Testing for exceptional convergence

The macroevolutionary landscape for *Anolis* thus appears to show numerous instances of convergence, but it is necessary to test whether the extent of convergence (i.e., c, the number of convergent shifts) is greater than expected by chance. Some convergence is expected by chance in a large radiation (*34*), and while the null distribution of c is unknown and will vary among data sets, we can obtain an appropriate null distribution using simulations under a model that lacks convergent adaptive peak shifts. We used two classes of null model, one accounting for the general tempo of trait evolution, and the other incorporating non-convergent adaptive peak shifts. All null model simulation analyses were carried out on the MCC phylogenetic tree and compared to the corresponding analysis of anole data.

First, we simulated 99 null data sets on the MCC tree using the trait-specific model described in Materials and Methods, Section 2. We ran the SURFACE algorithm on each of these data sets as we did for the anole data, and extracted the measures of the extent of convergence. Both the number ($c = 22$, $P = 0.01$) and proportion of convergent adaptive peak shifts ($c/k = 0.76$, $P = 0.01$) in anoles greatly exceeded the null expectation (Fig. 1B). The number and proportion of convergent peak shifts in *Anolis* also exceeded expectations when we repeated this analysis using 99 data sets simulated under each of the BM, EB, TM, and LD models (Fig. S5).

These null models do not include adaptive peak shifts in the generating process, and the model recovered by the forward phase of SURFACE included more peak shifts in *Anolis* than it did for these simulated data sets ($P = 0.01$). To account for the possibility that the large number of convergent shifts c was due simply to the large number of total shifts k, we analyzed data simulated under a generating model that included adaptive

peak shifts. We used the Hansen model from the final iteration of the forward phase of the analysis, preserving all features except for the positions of the optima. We calculated the mean and variance of the *k* optima estimated for each trait axis, and for each null model simulation we sampled new optima for each adaptive peak from the corresponding normal distribution. These null models thus preserve the values of σ^2 and α and the number and placement of peak shifts, but break up any tendency of optima to cluster in trait space beyond what is expected by chance. We used 99 such non-convergent null Hansen models to simulate trait data, and analyzed each data set with SURFACE. This analysis confirmed that the number and proportion of convergent adaptive peak shifts in the anole data were exceptionally high even when the presence of peak shifts was accounted for ($P = 0.02$ for both c and c/k; Fig. S5).

Finally, to evaluate whether the identified convergent adaptive peak shifts could explain the exceptional among-island faunal similarity in Greater Antillean *Anolis*, we compared our empirical estimate of among-island similarity (NND, from Materials and Methods, Section 3) to two additional "null" distributions. We generated the first null distribution from 999 data sets simulated using the non-convergent Hansen model described above, accounting for any tendency of peak shifts *per se* to result in more similarity than expected under the models already analyzed (BM, EB, TM, and LD). We confirmed that NND for anoles was exceptional compared to data generated under a non-convergent Hansen model ($P = 0.002$; Fig. S1). To obtain the second null distribution, we simulated 999 data sets using the final, convergent Hansen model estimated for our empirical data. Compared to this distribution, the empirical NND was not exceptional ($P = 0.160$; Fig. S1), indicating that our model of the macroevolutionary adaptive landscape can explain the among-island faunal similarity of Greater Antillean *Anolis*.

5. Model Adequacy, Uncertainty, and Sensitivity Testing

5a. Testing sensitivity to phylogenetic marker choice

We conducted all comparative analyses using mitochondrial DNA (mtDNA) phylogenies from Mahler et al. (*17*), which represent the most taxonomically complete estimates of phylogeny from a single type of data presently available for Greater Antillean anoles. However, phylogenetic data for 46 nuclear markers are also available for 61 species from the Greater Antilles from the analysis of Alföldi et al. (*36*). A key finding of that study was that phylogenetic analysis of nuclear DNA corroborates previous analyses based on mitochondrial DNA, a finding that we confirm applies to the relationships of the 61 species shared in the Mahler et al. (*17*) and Alföldi et al. (*36*) analyses. For this taxon set, the topology presented in Alföldi et al. differs from the MCC topology of Mahler et al. by only 13 nearest-neighbor interchanges, and the monophyly of all independently evolved traditional ecomorph lineages is supported in both trees.

The 61-species nuclear DNA sample is insufficient for testing for convergence among entire island radiations both because it is missing ecomorphologically distinct lineages (e.g., *Anolis occultus*, *A. sheplani* and *A. placidus*, *A. vermiculatus*, the *A. equestris* clade), and because SURFACE convergence parameter estimates are unlikely to be meaningful with highly incomplete species sampling (*20*). However, we can test whether the relatively minor differences between nuclear and mtDNA phylogeny estimates are likely to influence the results of tests for convergent evolution – i.e.,

whether best-fit models of convergent trait evolution differ fundamentally when estimated using nuclear DNA versus mtDNA phylogenies.

To determine whether nuclear and mtDNA phylogenies yield comparable convergence parameter estimates for *Anolis*, we conducted analyses on matching nuclear DNA and mtDNA phylogenies, pruned to contain only the 61 species shared by both. We analyzed the published *Anolis* phylogeny of Alföldi et al. (*36*), which was estimated using maximum likelihood analysis (GTR + gamma models, partitioned by locus) of a 19,987 bp alignment representing 46 nuclear loci for 93 species (91 *Anolis*, plus two outgroups). We estimated relative divergence times for this tree using RelTime (*41*). Branch lengths were estimated from the Alföldi et al. alignment (considering all sites with 75% or greater coverage), assuming a GTR + gamma substitution model, using the local clocks method with no merging of clock rates (this was the best-fit model). This chronogram was then pruned to include only the 61 species also present in the mtDNA phylogenies and rescaled to a root age of 50 MY.

We prepared analogous mtDNA chronograms from the 100-tree posterior sample of trees used for our main analyses. We pruned each of these 100-species chronograms to 61 species (removing species not in the nuclear tree), and rescaled it to 50 MY.

Next, for each tree, we phylogenetically prepared our morphological data (using the tree to phylogenetically size-correct all shape traits and conduct a phylogenetic PCA; trait loadings for these axes closely resembled those described in our main analyses), and analyzed the first four pPC axes. From the final model from each SURFACE analysis, we recorded the number of adaptive peak shifts, the total number of inferred adaptive peaks, the number of convergent adaptive peak shifts, and the number of convergent adaptive peaks.

The macroevolutionary parameters estimated for the 61-species nuclear data set are similar to those estimated using mtDNA (Fig. S6). All fall within the range of parameters estimated for the 100-tree posterior sample of mtDNA trees (differences all non-significant). Thus, despite the fact that sampling of nuclear DNA data is presently limited for *Anolis*, estimates of the evolutionary process obtained using mitochondrial phylogenetic data are concordant with those inferred from nuclear data.

5b. Assessing uncertainty in model estimation

We conducted two additional sets of analyses to assess whether uncertainty in stepwise model estimation has affected our conclusions about the macroevolutionary landscape in anoles. We first assessed the robustness of model selection at each step of the SURFACE algorithm, and then tested whether allowing the algorithm to explore alternative pathways to estimating a convergent landscape yielded superior and fundamentally different models.

Recent work has shown that Akaike's Information Criterion may lead to high error rates when used as a criterion for model selection in phylogenetic comparative analyses (*42*). To evaluate whether SURFACE had a tendency to accept new models with low statistical support, we conducted phylogenetic Monte Carlo simulations using the 'pmc' R package (*42*). At each iteration, we simulated 99 data sets under each of the current and previous Hansen models, then calculated statistical significance and power using log-likelihood differences added across traits. During the forward phase, new models were consistently a statistical improvement over preceding models (all $p \leq 0.06$),

and there was high power to support a more complex true model (0.94-1.0). We then conducted simulations for the backward phase, and found that aside from the final iteration ($P = 0.14$), all steps of this phase led to statistically significant improvements ($P = 0.01$) (note that both models compared during the final iteration strongly supported exceptional levels of convergence among island radiations of anoles; Table S4). Power to detect a model with more adaptive peak collapses was variable but generally lower during the backward phase (0.18-1.0), suggesting that the algorithm is at times conservative at identifying convergence during individual steps of the backward phase. These simulations indicate that AIC_c is effective at informing model choice during the steps of our analysis.

We then investigated the effect of algorithm path-dependence on our results. A potential drawback of stepwise model selection is that model choice during early steps affects the availability of models for comparison during subsequent steps; in some cases, this may preclude consideration of well-supported models. However, it is possible to relax path-dependence in model selection by allowing random selection from a candidate set of well-supported models at each step, rather than deterministically selecting the best model. By repeatedly analyzing a data set using such relaxed selection criteria, we are able to generate a set of model estimates with reduced path-dependence for comparison.

To assess whether support for our final model was influenced by path-dependence in the estimation procedure, we repeated our stepwise analysis 100 times using the MCC *Anolis* phylogeny, using an "alternative chains" approach. At each step, we identified all candidate models that were within 5 AIC_c units of the best model and met the $\Delta AIC_c < \Delta AIC_c$* criterion, and chose the position of the peak shift for that step by randomly selecting a model from this candidate set. The 100 resulting final models varied considerably in support (Fig. S7). Allowing selection of relatively poorly supported models at various steps led many runs to return comparatively poor final models, but many returned models with roughly equivalent, or even slightly better, AIC_c support compared to our standard final model.

We investigated whether macroevolutionary parameter estimates for well-supported alternative chains models differ from those estimated for our standard SURFACE model. For comparison, we defined a credible set containing all final models with AIC_c scores within 10 units of the standard SURFACE model. Twenty-six of the 100 alternative chains models met this criterion, including all models that performed better than the standard SURFACE model.

All well-supported alternative chains models were highly similar to the standard model, and all recovered nearly identical patterns of convergence for Greater Antillean *Anolis* (Table S5). Topological details of peak shift placement were also highly similar between the standard and credible alternative chains models. Nearly all branches found together on the same adaptive peak in the standard model were also found together in all alternative chains models (mean proportion of identical cells in pairwise peak co-occurrence matrix for all branches = 0.98; range = [0.96,1.0]). To illustrate using an example, we present the topological history of adaptive peak shifts and the positions of species and adaptive peaks in morphospace for the alternative chains model with the lowest AIC_c score out of all 100 such models estimated (Fig. S8). This model is nearly identical to the standard model, although it identifies a single additional instance of among-island convergence.

5c. Comparison of stepwise adaptive peak-shift and stepwise rate-shift models

The Hansen model estimated by SURFACE was strongly favored over a variety of simpler models of trait evolution, including Brownian motion, several models with declining evolutionary rate, and a single-peak Ornstein-Uhlenbeck model (Fig. S2). Evolutionary processes are unlikely to be homogeneous across entire radiations, and the complexity of multi-peak Hansen models and the exploration of model space could predispose our analysis to finding a model that fits the trait data well despite not representing the evolutionary process well. Thus, we compared our Hansen model to a model returned by a similar stepwise algorithm, traitMEDUSA (*24*), which uses stepwise AIC_c to fit models of trait evolution with multiple Brownian rate shifts, rather than multiple adaptive peak shifts.

We input our trait data and tree to traitMEDUSA, and allowed it to add rate shifts until the AIC_c stopped improving. We modified the AIC_c calculation in traitMEDUSA to be consistent with the way SURFACE calculates AIC_c. Namely, each new rate shift adds two parameters: a "shift" parameter and a rate parameter representing the rate multiplier applied to all traits. traitMEDUSA added a total of 15 Brownian rate shifts before the AIC_c stopped improving (Fig. S9). The resulting model fit better than any of the simple models (single peak OU, BM, EB, Time or Lineage Diversity models), but not nearly as well as the models returned by the forward and backward phases of SURFACE (Fig. S2). Thus, a paradigm of shifts between adaptive peaks (with constant rates of Brownian evolution and adaptation) provides a better fit to the anole data than one of shifts in the rate of stochastic evolution.

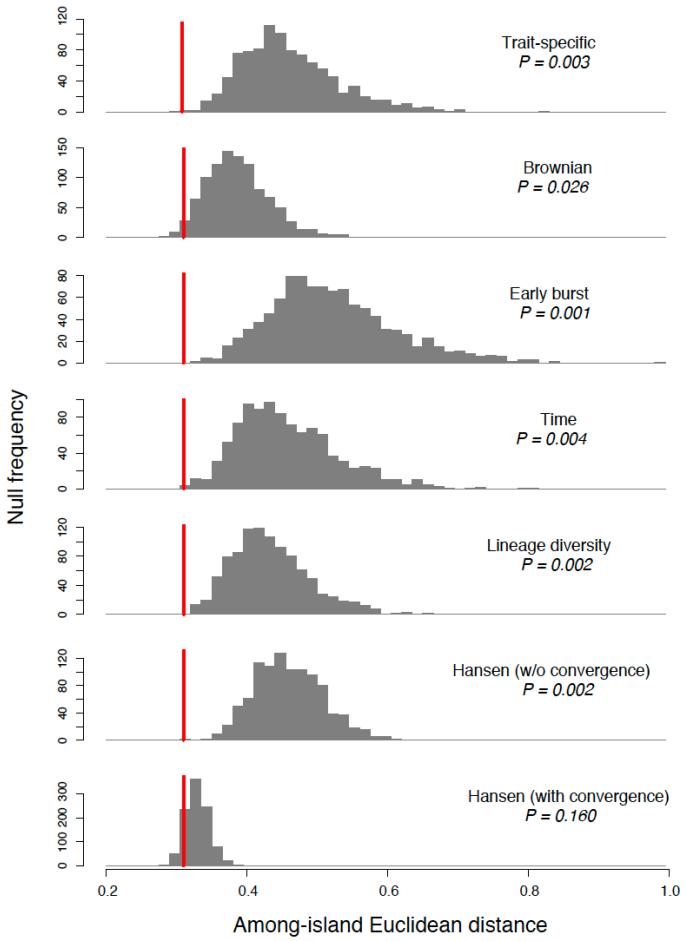

Fig. S1.

Among-island faunal similarity for Greater Antillean *Anolis* is greater than expected under several null models of evolution. We simulated under seven fitted models, including trait-specific, Brownian motion, early burst, time, lineage diversity, and Hansen models. We simulated under two Hansen models, both using parameters estimated for our empirical data by the SURFACE algorithm. The first Hansen model features peak shifts on the adaptive landscape, but lacks explicit convergence; the second (bottom panel) is parameterized using the final model that includes explicit convergence to shared adaptive peaks. The non-significance of the second Hansen model indicates that our model of convergent adaptive peak shifts can account for the observed among-island faunal similarity. Results for the trait-specific model were also depicted in Fig. 1A, but are shown here for comparison. Histograms represent simulated null distributions for the among-island nearest neighbor similarity statistic, with red lines indicating the empirical value. *P*-values reflect the probabilities of obtaining the empirical result under each null simulation model.

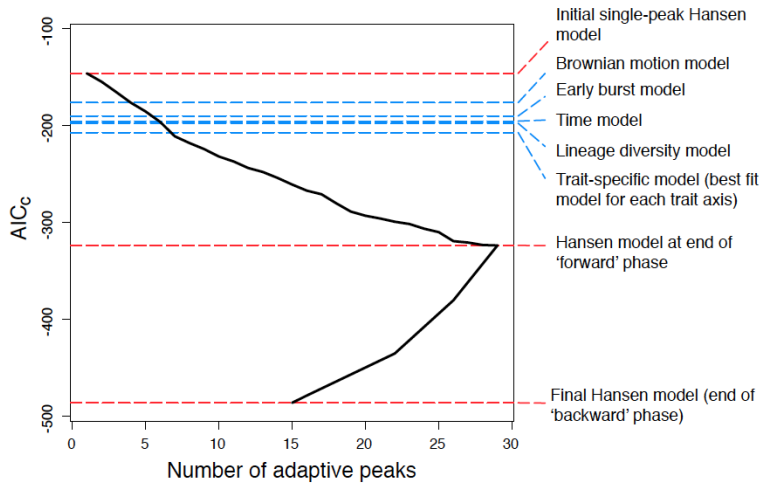

Fig. S2

Sequence of Hansen model improvement as the SURFACE algorithm proceeds through 'forward' and 'backward' stepwise phases for the Greater Antillean *Anolis* data set. Starting in the upper left portion of the plot, the black line traces change in model support (AIC_c) as new adaptive peak shifts are added to the model during the 'forward' phase, and then as similar peaks are collapsed during the 'backward' phase. Dashed lines indicate AIC_c values for the initial single-peak Hansen model, the model estimated at the end of the 'forward' phase, and the final model (all in red), as well as five alternative models that do not feature adaptive peaks (in blue; see text for description). Early in this sequence (by the addition of the 7^{th} distinct peak), the algorithm identifies adaptive landscape models that outperform all models lacking macroevolutionary peak shifts. The final model selected is characterized by extensive convergence on the adaptive landscape.

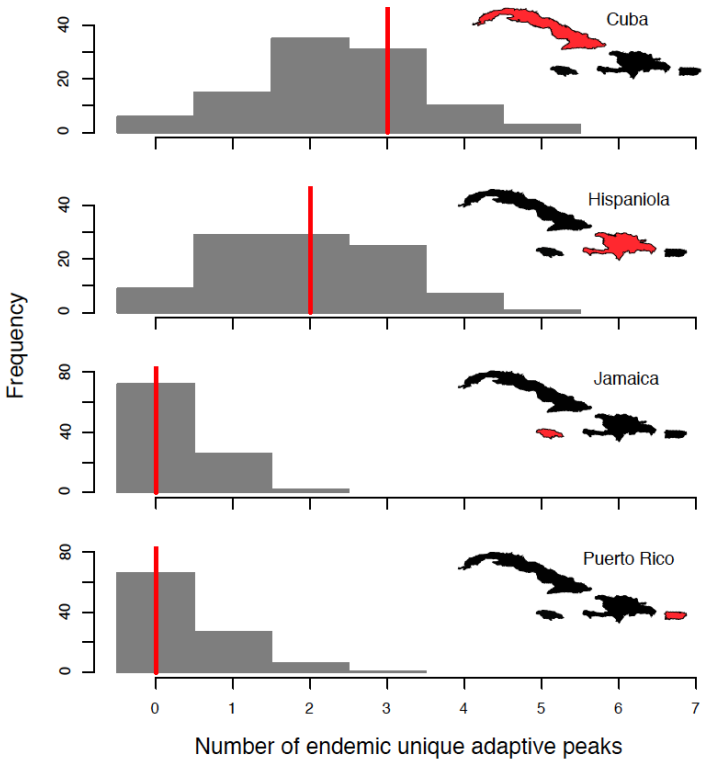

Fig. S3

The numbers of endemic unique adaptive peaks observed on each island in Greater Antillean *Anolis* (red lines) match expectations of the "area effect" from adaptive radiation theory (histograms). In *Anolis*, five endemic "unique" peaks were observed – three on Cuba, two on Hispaniola, and zero on the smaller islands of Jamaica and Puerto Rico. Histograms represent distributions of the expected number of endemic unique adaptive peaks on each island given its evolutionary diversity, and assuming that shifts to five unique peaks were phylogenetically random. The four Greater Antilles are illustrated to scale in each panel, with the corresponding island in red.

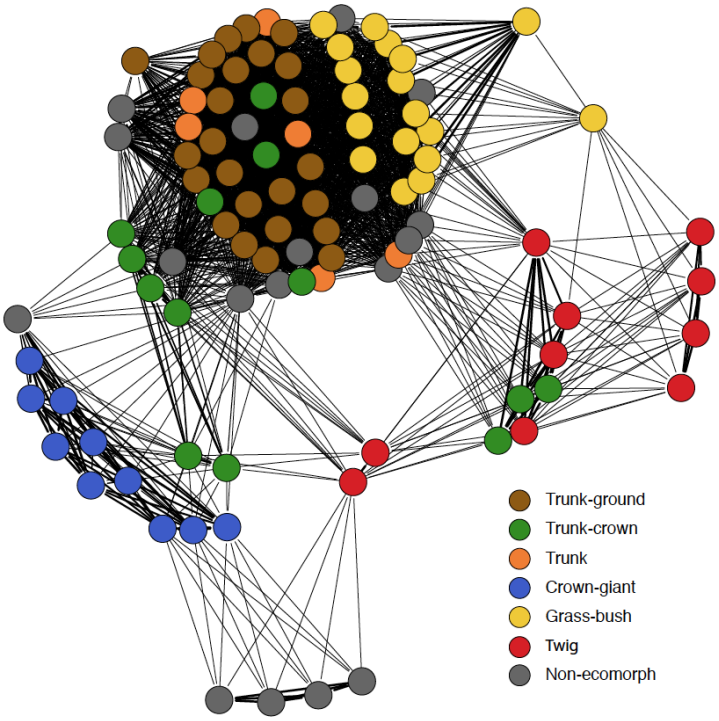

Fig. S4

Adaptive peak associations estimated from ecomorphology data by SURFACE are broadly concordant with *Anolis* ecomorph classifications. Edges in this graph connect pairs of species (nodes) if they occupy the same adaptive peak in any of 100 sampled Bayesian phylogenies, with edge thickness proportional to the number of phylogenies in which the pair shares an adaptive peak; nodes are arranged to illustrate peak co-occupation patterns, but their plot coordinates are arbitrary. Species are colored according to the traditional ecomorph classification presented in reference (*14*) (*pp. 411-420*) to show that members of the same ecomorph class tend to be attracted to the same adaptive peak. Note that traditional ecomorph classifications played no role in either the estimation of adaptive peaks or the generation of the graph. Also, because Hansen model adaptive peaks do not correspond directly to ecomorph classes, the colors in this figure do not correspond directly to those of Fig. 2.

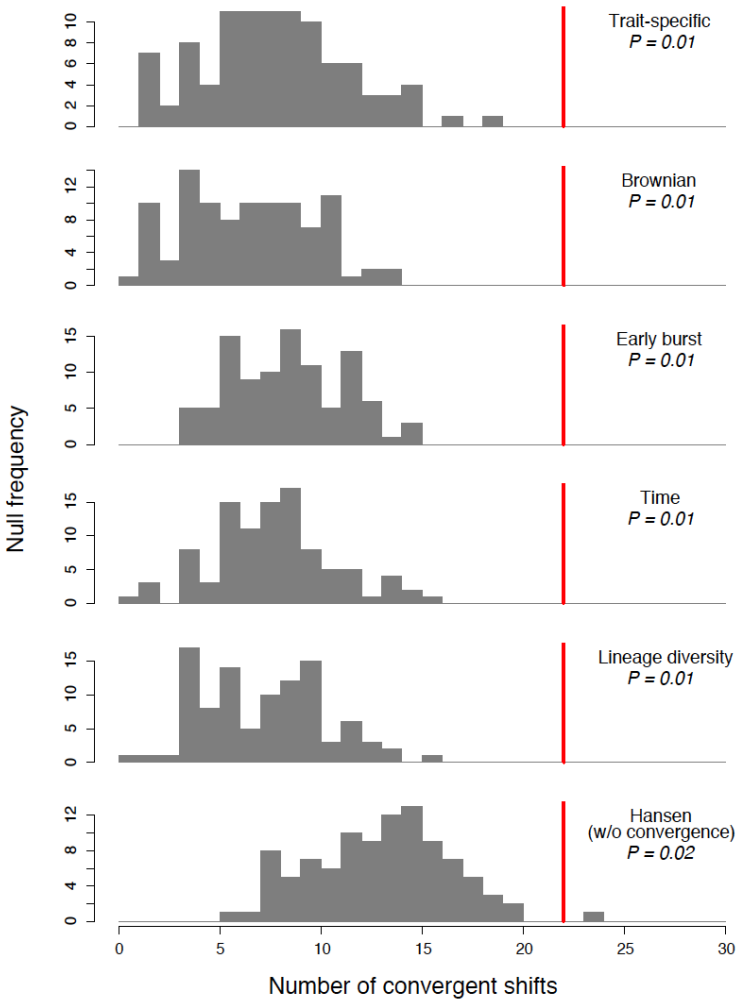

Fig. S5

Convergent adaptive peak shifts (*c*) occurred more frequently in Greater Antillean *Anolis* than expected under several null models of evolution. We simulated under six fitted models, including trait-specific, Brownian motion, early burst, time, lineage diversity, and Hansen models. Results for the trait-specific model were also depicted in Fig. 1B, but are shown here for comparison. Histograms represent simulated null distributions for the number of convergent peak shifts, with red lines indicating the empirical value. *P*-values reflect the probabilities of obtaining the empirical result under each null simulation model.

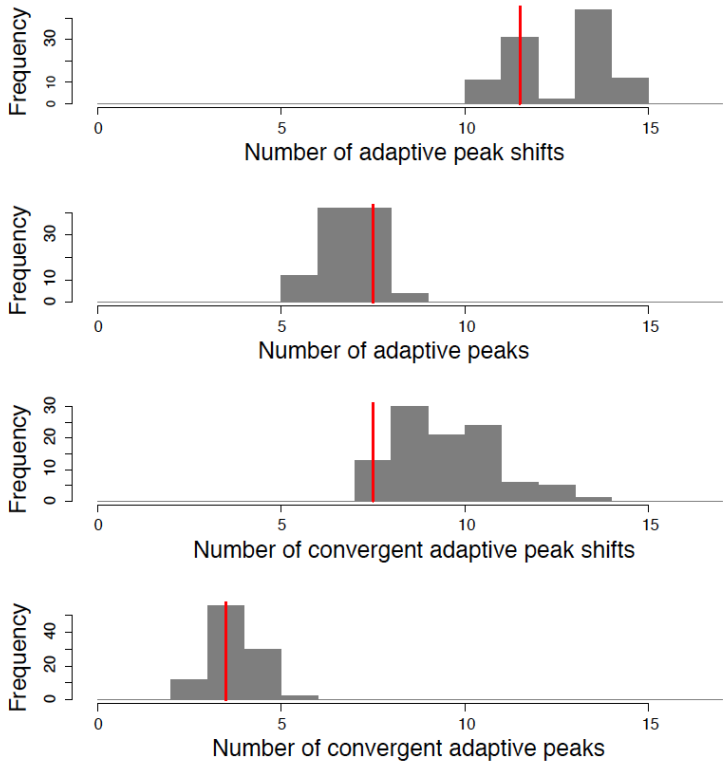

Fig. S6

Final Hansen model parameters estimated for 61 species of Greater Antillean *Anolis* using a 46 locus nuclear phylogeny (red lines) versus a mtDNA phylogeny (gray histograms). Histograms represent parameter estimates from analyses conducted on the 100-tree mtDNA posterior sample described above. For the nuclear analysis, parameters describing the shape of macroevolutionary adaptive landscape (number of adaptive peaks), as well as the specific history of convergent evolution on this landscape (numbers of adaptive peak shifts, convergent adaptive peak shifts, and convergent adaptive peaks) lie within the range of estimates obtained for trees across the mtDNA posterior distribution. Note that because these analyses exclude many distinctive lineages, we expect them to recover a highly incomplete history of adaptive peak shifts and convergence for Greater Antillean *Anolis*; nonetheless, they reveal that the estimation of complex Hansen models is robust to phylogenetic marker choice.

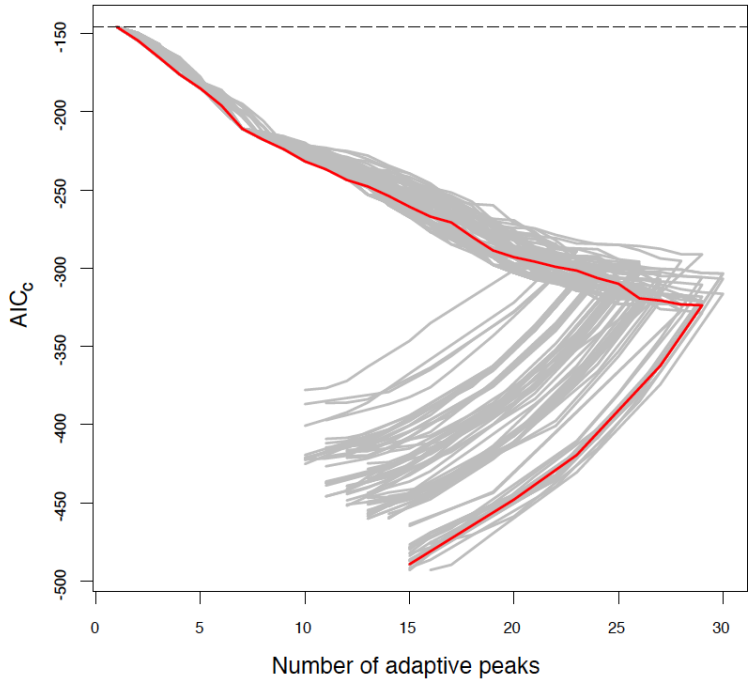

Fig. S7

Sequence of Hansen model improvement for the standard SURFACE analysis of Greater Antillean *Anolis* data (red line), and for 100 "alternative chains" analyses of the same data (gray lines). Starting in the upper left portion of the plot, lines trace improvement in model support (measured using AIC_c; dashed line indicates value for the starting model) as new adaptive peaks are added to the model during the 'forward' phase, and then as similar peaks are collapsed during the 'backward' phase.

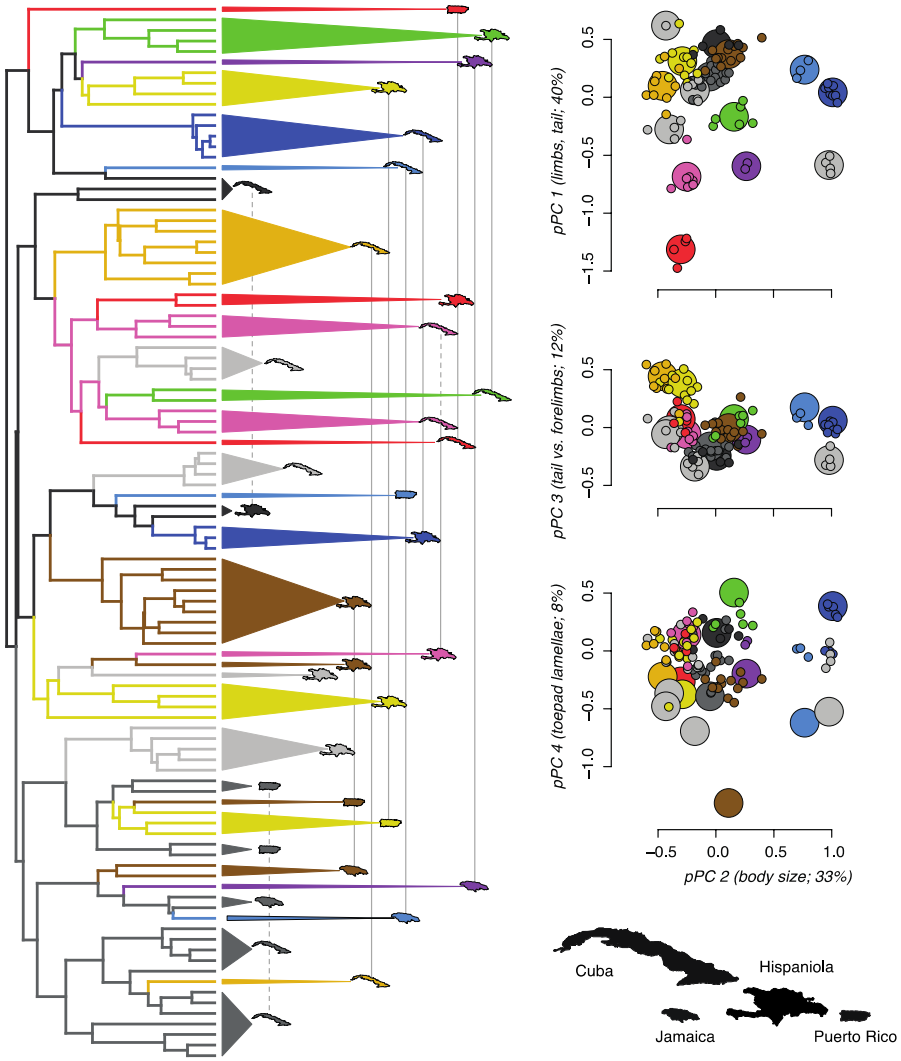

Fig. S8

Estimate of the Greater Antillean *Anolis* macroevolutionary adaptive landscape for the "alternative chains" model with the lowest AIC_c score (out of 100 runs of the "alternative chains" SURFACE algorithm). This model is nearly identical to the model returned by the standard SURFACE algorithm (compare to Fig. 2). It contains the same number of adaptive peak shifts (k=29), but identifies one additional instance of among-island convergence (adaptive peak denoted in pink; convergence is among twig-dwelling anoles from Hispaniola and Cuba). Colors and shapes are as in Fig. 2.

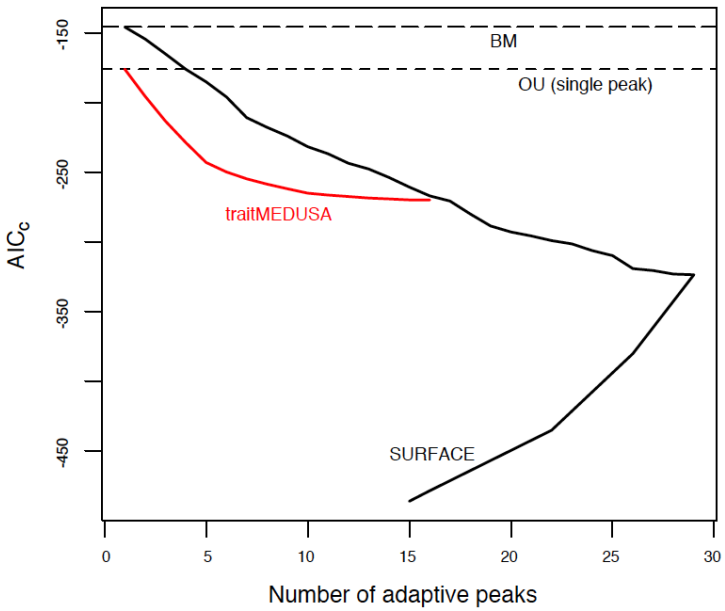

Fig. S9

Comparison of sequences of model improvement for the stepwise SURFACE analysis of Greater Antillean *Anolis* data (black line), and a stepwise traitMEDUSA analysis of the same data (red line). Starting in the upper left portion of the plot, lines trace improvement in model support (measured using AIC_c) with each additional step in the algorithm. The simpler traitMEDUSA models outperform SURFACE models for the sequential addition of 15 shifts, but cease to improve further as additional shifts are added. Both the 'forward' and 'backward' phase SURFACE models strongly outperform the best estimated traitMEDUSA model.

Table S1 (separate file).

Traits, loadings, and variance explained for the axes of a phylogenetic principal component analysis (pPCA) of 11 ecomorphological traits using the MCC chronogram from the Bayesian posterior distribution of phylogenetic trees. pPC axes 1-4 explained 93% of trait variation, and were strongly correlated with our raw variables. All analyses were conducted using a morphospace defined by these four axes.

Table S2 (separate file).

Principal component scores for the axes of a pPCA of 11 ecomorphological traits using the MCC chronogram from the Bayesian posterior distribution of phylogenetic trees. pPC axes 1-4 explained 93% of trait variation, and were strongly correlated with our raw variables. All analyses were conducted using a morphospace defined by these four axes.

Table S3.

Comparison of the fit of four models of continuous trait evolution for each pPC axis in the empirical morphospace for Greater Antillean *Anolis*, using the MCC tree. Models include Brownian motion (BM), early burst (EB), time (TM), and lineage diversity (LD). For all models, we report the number of parameters (np), the starting rate of stochastic evolution (σ^2_0), the log likelihood score, and a measure of relative model fit (ΔAIC_c). For the EB model, we also report the exponential rate decline parameter (*r*), and for the TM and LD models, we report linear rate decline parameters (Ψ) corresponding to time or the accumulated diversity of sympatric lineages, respectively. For the BM model, there is no rate decline, and σ^2_0 is the best-fit evolutionary rate for the entire radiation. For each trait axis, the lowest ΔAIC_c score (0 in each case; indicated in bold) represents the best-fit model, and this model was used to simulate null trait axes. Parameters and model selection results presented here for the MCC tree are representative of those for the 100 trees from the posterior sample, although in some cases, different models were favored for a given trait axis in different trees (data available upon request). This variation was minor, and did not influence any results.

Trait	**Model**	**np**	$\boldsymbol{\sigma^2_0}$	$\boldsymbol{\Psi}$	***r***	**log(L)**	$\boldsymbol{\Delta AIC_c}$
pPC 1	BM	2	3.3E-03	-	-	-13.7	19.0
	EB	3	3.2E-02	-	-6.8E-02	-5.2	4.2
	TM	3	7.3E-03	-1.4E-04	-	-3.1	0.0
	LD	3	4.7E-03	-8.3E-05	-	-8.0	9.7
pPC 2	BM	2	2.7E-03	-	-	-4.7	10.1
	EB	3	4.6E-03	-	-1.4E-02	-4.3	11.5
	TM	3	4.7E-03	-6.4E-05	-	-3.6	10.1
	LD	3	4.3E-03	-8.4E-05	-	1.4	0.0
pPC 3	BM	2	1.0E-03	-	-	45.6	0.7
	EB	3	2.0E-03	-	-1.9E-02	46.3	1.4
	TM	3	1.6E-03	-2.0E-05	-	46.5	1.1
	LD	3	1.3E-03	-1.7E-05	-	47.0	0.0
pPC 4	BM	2	6.2E-04	-	-	69.1	0.9
	EB	3	1.5E-03	-	-2.5E-02	70.5	0.0
	TM	3	9.5E-04	-1.1E-05	-	70.2	0.6
	LD	3	7.7E-04	-8.3E-06	-	70.5	0.1

Table S4.

Convergence parameters for models estimated during the last two steps of the SURFACE algorithm. The final model was favored by 7.51 AIC_c units, but data simulated under the two models exhibited moderate overlap ($P = 0.13$). However, the two models yield nearly identical estimates of evolution on the macroevolutionary adaptive landscape, and both show support for exceptional convergence among Greater Antillean *Anolis* radiations.

	Penultimate model	**Final model**
Adaptive peak shifts	29	29
Convergent adaptive peak shifts	21	22
Adaptive peaks	16	15
Convergent adaptive peaks	8	8
Convergence fraction (convergent peak shifts / total peak shifts)	0.72	0.76
Average number of lineages converging to each shared adaptive peak	2.6	2.8
Fraction of convergent peaks with lineages from multiple islands	0.88	0.88

Table S5.

Convergence parameters for the final Hansen model estimated by the standard stepwise algorithm, and for a set of well-supported models from 100 runs that explore alternative chains (included models are all within 10 AIC_c units of the standard model). Analyses were conducted using the MCC *Anolis* phylogeny. For the 26 alternative chains models, we present mean parameter values, with ranges in parentheses.

	Standard model	**Alternative chains credible model set (26 models)**
Adaptive peak shifts	29	29.1 (29-30)
Convergent adaptive peak shifts	22	22.8 (22-24)
Adaptive peaks	15	15.1 (15-16)
Convergent adaptive peaks	8	8.8 (8-10)
Convergence fraction (convergent peak shifts / total peak shifts)	0.76	0.78 (0.76-0.80)
Average number of lineages converging to each shared adaptive peak	2.8	2.6 (2.4-2.8)
Fraction of convergent peaks with lineages from multiple islands	0.88	0.95 (0.88-1.0)

Author Contributions: D.L.M., T. I., L.J.R., and J.B.L. conceived the project. D.L.M. collected the data and, with T. I. and L.J.R., conducted the analyses. D.L.M., T. I., L.J.R., and J.B.L. wrote the paper.

References and Notes

1. S. Gavrilets, A. Vose, Dynamic patterns of adaptive radiation. *Proc. Natl. Acad. Sci. U.S.A.* **102**, 18040–18045 (2005). doi:10.1073/pnas.0506330102 Medline

2. D. Schluter, *The Ecology of Adaptive Radiation* (Oxford Univ. Press, Oxford, 2000).

3. G. G. Simpson, *Tempo and Mode in Evolution* (Columbia Univ. Press, New York, 1944).

4. E. I. Svensson, R. Calsbeek, Eds., *The Adaptive Landscape in Evolutionary Biology* (Oxford Univ. Press, Oxford, 2012)

5. B. Frédérich, L. Sorenson, F. Santini, G. J. Slater, M. E. Alfaro, Iterative ecological radiation and convergence during the evolutionary history of damselfishes (Pomacentridae). *Am. Nat.* **181**, 94–113 (2013). doi:10.1086/668599 Medline

6. R. Gillespie, Community assembly through adaptive radiation in Hawaiian spiders. *Science* **303**, 356–359 (2004). doi:10.1126/science.1091875 Medline

7. T. J. Givnish, in *The Biology of Biodiversity*, M. Kato, Ed. (Springer-Verlag, Tokyo, 1999), pp. 67–90.

8. M. Muschick, A. Indermaur, W. Salzburger, Convergent evolution within an adaptive radiation of cichlid fishes. *Curr. Biol.* **22**, 2362–2368 (2012). doi:10.1016/j.cub.2012.10.048 Medline

9. M. L. J. Stiassny, A. Meyer, Cichlids of the Rift Lakes. *Sci. Am.* **280**, 64–69 (1999). doi:10.1038/scientificamerican0299-64

10. K. A. Young, J. Snoeks, O. Seehausen, Morphological diversity and the roles of contingency, chance and determinism in African cichlid radiations. *PLoS ONE* **4**, e4740 (2009). doi:10.1371/journal.pone.0004740 Medline

11. Past studies of convergence between species-rich radiations have been selective in scope and have not compared entire radiations. Even lineages diversifying randomly under genetic drift will generate many convergent pairs (*34*), as will radiations adapting on a labile macroevolutionary landscape (*27*). Much of the diversity unsampled by past studies may be nonconvergent, so that different radiations may share many convergent species pairs while being unexceptionally similar at the whole-radiation scale.

12. M. L. Cody, H. A. Mooney, Convergence versus nonconvergence in Mediterranean-climate ecosystems. *Annu. Rev. Ecol. Syst.* **9**, 265–321 (1978). doi:10.1146/annurev.es.09.110178.001405

13. R. Kassen, Toward a general theory of adaptive radiation: Insights from microbial experimental evolution. *Ann. N. Y. Acad. Sci.* **1168**, 3–22 (2009). doi:10.1111/j.1749-6632.2009.04574.x Medline

14. J. B. Losos, *Lizards in an Evolutionary Tree: Ecology and Adaptive Radiation of Anoles* (Univ. of California Press, Berkeley, CA, 2009).

15. E. E. Williams, in *Lizard Ecology: Studies of a Model Organism*, R. B. Huey, E. R. Pianka, T. W. Schoener, Eds. (Harvard Univ. Press, Cambridge, MA, 1983), pp. 326–370.

16. J. B. Losos, T. R. Jackman, A. Larson, K. de Queiroz, L. Rodríguez-Schettino, Contingency and determinism in replicated adaptive radiations of island lizards. *Science* **279**, 2115–2118 (1998). doi:10.1126/science.279.5359.2115 Medline

17. D. L. Mahler, L. J. Revell, R. E. Glor, J. B. Losos, Ecological opportunity and the rate of morphological evolution in the diversification of Greater Antillean anoles. *Evolution* **64**, 2731–2745 (2010). doi:10.1111/j.1558-5646.2010.01026.x Medline

18. Information on materials and methods is available as supplementary material on *Science* Online.

19. L. J. Harmon, J. B. Losos, T. J. Davies, R. G. Gillespie, J. L. Gittleman, W. B. Jennings, K. H. Kozak, M. A. McPeek, F. Moreno-Roark, T. J. Near, A. Purvis, R. E. Ricklefs, D. Schluter, J. A. Schulte II, O. Seehausen, B. L. Sidlauskas, O. Torres-Carvajal, J. T. Weir, A. Ø. Mooers, Early bursts of body size and shape evolution are rare in comparative data. *Evolution* **64**, 2385–2396 (2010). Medline

20. T. Ingram, D. L. Mahler, SURFACE: Detecting convergent evolution from comparative data by fitting Ornstein-Uhlenbeck models with stepwise Akaike Information Criterion. *Methods Ecol. Evol*. **4**, 416–425 (2013).

21. M. A. Butler, A. A. King, Phylogenetic comparative analysis: A modeling approach for adaptive evolution. *Am. Nat.* **164**, 683–695 (2004). doi:10.1086/426002

22. T. F. Hansen, Stabilizing selection and the comparative analysis of adaptation. *Evolution* **51**, 1341 (1997). doi:10.2307/2411186

23. M. E. Alfaro, F. Santini, C. Brock, H. Alamillo, A. Dornburg, D. L. Rabosky, G. Carnevale, L. J. Harmon, Nine exceptional radiations plus high turnover explain species diversity in jawed vertebrates. *Proc. Natl. Acad. Sci. U.S.A.* **106**, 13410–13414 (2009). doi:10.1073/pnas.0811087106 Medline

24. G. H. Thomas, R. P. Freckleton, MOTMOT: Models of trait macroevolution on trees. *Methods Ecol. Evol* **3**, 145–151 (2012). doi:10.1111/j.2041-210X.2011.00132.x

25. G. L. Conte, M. E. Arnegard, C. L. Peichel, D. Schluter, The probability of genetic parallelism and convergence in natural populations. *Proc. Biol. Sci.* **279**, 5039–5047 (2012). doi:10.1098/rspb.2012.2146 Medline

26. G. Pinto, D. L. Mahler, L. J. Harmon, J. B. Losos, Testing the island effect in adaptive radiation: Rates and patterns of morphological diversification in Caribbean and mainland *Anolis* lizards. *Proc. Biol. Sci.* **275**, 2749–2757 (2008). doi:10.1098/rspb.2008.0686 Medline

27. T. F. Hansen, in *The Adaptive Landscape in Evolutionary Biology*, E. Svensson, R. Calsbeek, Eds. (Oxford Univ. Press, Oxford, 2012), pp. 205–226.

28. S. Estes, S. J. Arnold, Resolving the paradox of stasis: Models with stabilizing selection explain evolutionary divergence on all timescales. *Am. Nat.* **169**, 227–244 (2007). doi:10.1086/510633 Medline

29. J. C. Uyeda, T. F. Hansen, S. J. Arnold, J. Pienaar, The million-year wait for macroevolutionary bursts. *Proc. Natl. Acad. Sci. U.S.A.* **108**, 15908–15913 (2011). doi:10.1073/pnas.1014503108 Medline

30. Y. Kisel, T. G. Barraclough, Speciation has a spatial scale that depends on levels of gene flow. *Am. Nat.* **175**, 316–334 (2010). doi:10.1086/650369 Medline

31. D. L. Rabosky, R. E. Glor, Equilibrium speciation dynamics in a model adaptive radiation of island lizards. *Proc. Natl. Acad. Sci. U.S.A.* **107**, 22178–22183 (2010). doi:10.1073/pnas.1007606107 Medline

32. S. J. Gould, *Wonderful Life: The Burgess Shale and the Nature of History* (Norton, New York, 1989).

33. C. E. Wagner, L. J. Harmon, O. Seehausen, Ecological opportunity and sexual selection together predict adaptive radiation. *Nature* **487**, 366–369 (2012). doi:10.1038/nature11144 Medline

34. C. T. Stayton, Is convergence surprising? An examination of the frequency of convergence in simulated datasets. *J. Theor. Biol.* **252**, 1–14 (2008). doi:10.1016/j.jtbi.2008.01.008 Medline

35. A. J. Drummond, A. Rambaut, BEAST: Bayesian evolutionary analysis by sampling trees. *BMC Evol. Biol.* **7**, 214 (2007). doi:10.1186/1471-2148-7-214 Medline

36. J. Alföldi, F. Di Palma, M. Grabherr, C. Williams, L. Kong, E. Mauceli, P. Russell, C. B. Lowe, R. E. Glor, J. D. Jaffe, D. A. Ray, S. Boissinot, A. M. Shedlock, C. Botka, T. A. Castoe, J. K. Colbourne, M. K. Fujita, R. G. Moreno, B. F. ten Hallers, D. Haussler, A. Heger, D. Heiman, D. E. Janes, J. Johnson, P. J. de Jong, M. Y. Koriabine, M. Lara, P. A. Novick, C. L. Organ, S. E. Peach, S. Poe, D. D. Pollock, K. de Queiroz, T. Sanger, S. Searle, J. D. Smith, Z. Smith, R. Swofford, J. Turner-Maier, J. Wade, S. Young, A. Zadissa, S. V. Edwards, T. C. Glenn, C. J. Schneider, J. B. Losos, E. S. Lander, M. Breen, C. P. Ponting, K. Lindblad-Toh, The genome of the green anole lizard and a comparative analysis with birds and mammals. *Nature* **477**, 587–591 (2011). doi:10.1038/nature10390 Medline

37. L. J. Revell, Size-correction and principal components for interspecific comparative studies. *Evolution* **63**, 3258–3268 (2009). doi:10.1111/j.1558-5646.2009.00804.x Medline

38. L. J. Revell, phytools: An R package for phylogenetic comparative biology (and other things). *Methods Ecol. Evol.* **3**, 217–223 (2012). doi:10.1111/j.2041-210X.2011.00169.x

39. E. Paradis, J. Claude, K. Strimmer, APE: Analyses of phylogenetics and evolution in R language. *Bioinformatics* **20**, 289–290 (2004). doi:10.1093/bioinformatics/btg412 Medline

40. L. J. Harmon, J. T. Weir, C. D. Brock, R. E. Glor, W. Challenger, GEIGER: Investigating evolutionary radiations. *Bioinformatics* **24**, 129–131 (2008). doi:10.1093/bioinformatics/btm538 Medline

41. K. Tamura, F. U. Battistuzzi, P. Billing-Ross, O. Murillo, A. Filipski, S. Kumar, Estimating divergence times in large molecular phylogenies. *Proc. Natl. Acad. Sci. U.S.A.* **109**, 19333–19338 (2012). doi:10.1073/pnas.1213199109 Medline

42. C. Boettiger, G. Coop, P. Ralph, Is your phylogeny informative? Measuring the power of comparative methods. *Evolution* **66**, 2240–2251 (2012). doi:10.1111/j.1558-5646.2011.01574.x Medline